

# A Structurally Enhanced Neck Exoskeleton to Assist with Head-Neck Motion

1<sup>st</sup> David Demaree  
Dept. of Mechanical Engineering  
University of Utah  
Salt Lake City, UT 84112  
david.demaree@utah.edu

2<sup>nd</sup> Haohan Zhang\*  
Dept. of Mechanical Engineering  
University of Utah  
Salt Lake City, UT 84112  
haohan.zhang@utah.edu

**Abstract**—This paper presents the design of a neck exoskeleton to assist with head-neck motion for patients with amyotrophic lateral sclerosis (ALS). Motor neuron degeneration caused by ALS can lead to neck muscle weakness, resulting in head drop (chin-on-chest posture). Current treatment using static neck collars is inadequate because these collars completely immobilize the head. A powered neck exoskeleton (Columbia exoskeleton) was previously developed to assist with head-neck movements but its structural limitations hindered its usability for patients with severe head drop. In this paper, we introduce the Utah neck exoskeleton which improved the structural stability of the previous Columbia design by (1) optimizing the transmission efficiency and range of motion, and (2) using more precise mechanical components. We quantified the structural stability of the Utah neck exoskeleton and demonstrated its usability with a healthy volunteer. The results show that the Utah neck exoskeleton has a suitable structure to potentially assist with head-neck movements for patients with severe ALS head drop.

**Index Terms**—Wearable Robotics, Neck Exoskeletons, Optimization, Head Drop, Amyotrophic Lateral Sclerosis

## I. INTRODUCTION

Amyotrophic lateral sclerosis (ALS) is a neurodegenerative disease. Respiratory failure is the leading cause of death, which is often foreshadowed by neck muscle weakness [1], [2]. Difficulties in swallowing, speaking, and eating are common [3], [4]. Neck muscle weakness leads to fatigue from supporting the head. In severe cases, the head completely drops, resulting in a ‘chin-on-chest’ posture. An estimated 5% of ALS patients suffer from severe head drop [5]. Because head posture affects swallowing and breathing, poor posture makes it more challenging to eat, speak, and breathe [6]. Beyond physical considerations, patients with head drop face difficulty in social situations as head drop makes it more difficult to speak and make eye contact during a conversation.

Current treatment for head drop is limited and static neck collars are primarily used [7]. These collars are designed to support the head at the chin which can restrict speaking, swallowing, and breathing. Additionally, these static collars do not accommodate voluntary movements. It is, therefore,

DD is a Masters student and HZ is an Assistant Professor. Both authors are affiliated with the Department of Mechanical Engineering and the Robotics Center at the University of Utah.

\*Corresponding author.

not surprising to see that many ALS patients prefer alternative strategies such as using multiple travel pillows to support the head or relying on the headrest of a reclining wheelchair. These patient-initiated preferences highlight a critical unmet need in current treatment using static neck collars. Recently, there have been some improvements to static neck collars [8]; however, none are capable of providing assistive torques.

Previously, we developed the world’s first neck exoskeleton at Columbia University using a novel parallel mechanism [9], [10]. This powered device has three degrees-of-freedom and was optimized to couple natural rotations with small translations of the head. While it allowed for a large range of head-neck rotation ( $\sim 70\%$ ), the Columbia exoskeleton has only been able to assist with motions in mild-to-moderate head drop patients [11]. For patients with complete head drop (severe cases), preliminary testing suggested that the Columbia exoskeleton cannot consistently support the full weight of the head ( $\sim 5$  kg [12]); despite adequate torques applied by the actuators. There are two major causes: (1) the prototype was made of low-profile mechanical components resulting in loose fitting jointed parts and bending of linkages, and, more importantly, (2) the force transmission from the actuated joints to the end-effector, governed by a Jacobian matrix, was inefficient at multiple head poses. There have been other design ideas for enabling head-neck movements, proposed by other groups [13]–[16]. While these concepts are interesting, most of these devices are bulky and none of them have yet been evaluated by patients with head drop.

In this paper, we present a new neck exoskeleton (Utah neck exoskeleton) to address the limitations in the Columbia design. The main contribution of this paper is attaining an optimized design that simultaneously maximizes the force transmission efficiency and the workspace of the exoskeleton through a multi-objective optimization. Additionally, a prototype that realizes this optimal design is built using structurally improved linkages and joints. Compared to the Columbia exoskeleton, the structural stability of the Utah exoskeleton is significantly improved, as shown in a bench-top experiment. Additionally, feasibility of protocol for a future patient study using the Utah exoskeleton is evaluated through demonstration on a single healthy volunteer.

## II. METHODS

### A. Background

We first briefly review our previous work to provide an adequate background of the neck exoskeleton. In the kinematic model (Figure 1) [9], which is shared by both the Columbia and the Utah exoskeletons, three parallel chains of linkages connect the base (attached to the shoulders) and the end-effector (attached to the head). Each chain consists of two revolute joints ( $B_i$  and  $M_i$ ) and one spherical joint ( $A_i$ ). Additionally, the axes of the two revolute joints within a chain intersect at a stationary point ( $C_i$ ). The locations of these intersecting points govern the rotation-translation coupling of the end-effector. As a special case, when these three points coincide, the mechanism becomes a spherical mechanism in which the end-effector purely rotates about the intersecting point [17].

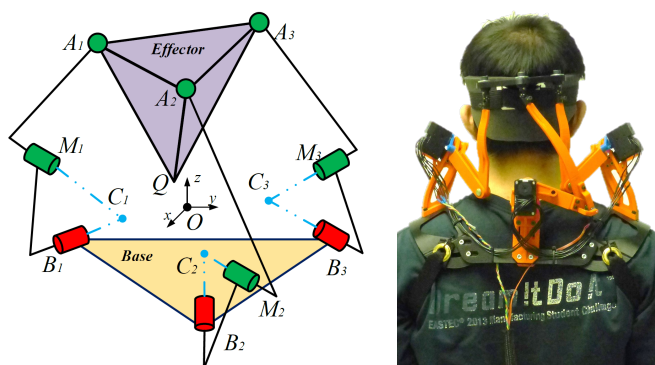


Fig. 1. (Left) Schematics of the kinematic model of the neck exoskeleton. The end-effector and middle joints (green) are passive spherical and revolute joints, respectively. The base joints (red) are actuated. (Right) The Columbia exoskeleton worn by a healthy volunteer.

Previously, the Columbia exoskeleton was optimized to maximize its range of rotation while accommodating the small translations of the head. The nature of this coupling was observed from recording the head-neck motion data of a healthy subject [9]. A two-step optimization was used: the locations of the intersecting points  $C_i$  were first optimized to best fit the rotation-translation coupling in the biomechanical data. This was followed by a hierarchical random search for the remaining geometric parameters, including the link lengths and the joint locations, to achieve a design that maximizes the ranges of rotation of the end-effector in the three anatomical planes (i.e., sagittal, frontal, and transverse planes).

The base revolute joints of the exoskeleton are actuated by motors, which provide torques to balance the external load applied on the end-effector (i.e., gravitational torque of the head). The required motor torques can be related to the external load through a Jacobian matrix which is determined by the configuration of the exoskeleton [18]. The condition number of the Jacobian matrix is a well established means to evaluate the performance of transmission at a given robot configuration [19], [20]. An ideal value for the condition number of a Jacobian matrix is 1. A large condition number (i.e., ill-conditioned) indicates a poor transmission from the

joint to the end-effector at a pose. If ill-conditioned, the end-effector can be easily perturbed from the nominal pose even with large motor torques. Despite a large range of rotations, the transmission efficiency of the Columbia exoskeleton is insufficient to support the full weight of the head for complete head drop at multiple head poses.

### B. Optimization

In this paper, the goal is to optimize the exoskeleton to simultaneously achieve large ranges of rotation and transmission efficiency. Because the translation-rotation coupling had previously been optimized to fit the biomechanical data, the locations of the intersecting points  $C_i$  were retained from the Columbia design. A constraint for symmetry about the sagittal plane was imposed for aesthetic reasons. Overall, there are 10 parameters to be optimized: referring to Figure 1, the coordinates of the base joints,  $B_i$ , in the inertial frame; coordinates of the spherical joint,  $A_i$ , in the end-effector frame; and lengths of the lower links. The lengths of the upper links are not included because they depend on other parameters in the kinematic model [9].

The metric for evaluating the range of motion was chosen to be a combination of the ranges of rotation about the vertical axis (axial rotation) and the lateral axis (flexion-extension), which are responsible for most of the head-neck rotations during daily tasks. The metric chosen to evaluate the transmission efficiency was the condition number of the Jacobian matrix at the upright pose, around which most daily head-neck movements occur.

The cost function was formulated as a weighted sum of the two objectives (i.e., range of motion and transmission efficiency):

$$c = w_1 g_1 + w_2 g_2,$$

where  $w_1$  and  $w_2$  are the weights for the normalized range of motion ( $g_1$ ) and the reciprocal of the condition number of the Jacobian matrix at the upright neutral pose ( $g_2$ ), respectively. Because the condition number is between 1 and  $\infty$ , its reciprocal ( $g_2$ ) is a quantity between 0 and 1. The ranges of motion (measured in degrees) were normalized with respect to  $180^\circ$  to result in a quantity between 0 and 1 for ( $g_1$ ). This formulation ensures that the cost,  $c$ , will be between 0 and 1. Weights  $w_1$  and  $w_2$  are tuned based on trial and error to yield a well balanced neck-brace design; and chosen to be 0.35 and 0.65, respectively.

We used a genetic algorithm to perform the optimization. The geometric parameters were encoded into a one-dimensional array (gene). Each parameter has a fixed range which was chosen to maintain a reasonable overall size and keep the field of view unobstructed. The algorithm is described as follows:

**Initialization:** The gene of an ‘individual’ is first randomly produced, following a uniform distribution, from the ranges of the parameters. If this individual also satisfies the kinematic equations of the neck exoskeleton (i.e., a feasible robot can be constructed), then this individual is introduced in the initial ‘population’. An initial population of 20 individuals was created.

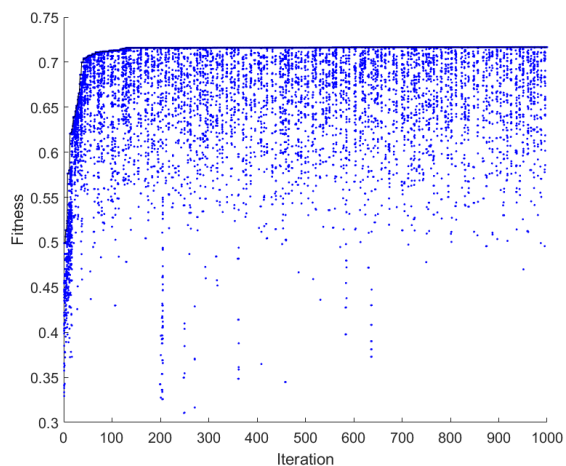


Fig. 2. Evolutionary fitness history. Blue dots represent the fitness of each generated exoskeleton design.

**Iteration:** After initialization, the evolution process begins. In each generation, the iteration process is as follows:

**Recombination:** Individuals are randomly paired to ‘breed’. For each pair (‘parents’), a crossover point is randomly chosen following a uniform distribution and their genes are swapped at that point. Two ‘children’ are produced.

**Mutation:** Each parameter in a ‘child’ has a mutation probability of 6%. Mutation occurs by generating a random number from a normal distribution centered at the current value ( $\sigma=10\text{mm}$ ).

**Selection:** The new population (parents plus children) is ranked based on fitness using the cost function. The best 20, plus the new offspring, are kept into the next generation. The new offspring are protected for one generation regardless of their cost to help regulate the diversity in the population. To prevent the ‘overgrowth’ of the population (for a manageable computation), the population size is limited to 100.

**Termination:** The algorithm ends after 1000 iterations. As shown in Figure 2, the ‘fitness’ of the population improved drastically within the first 200 generations, with only minor improvements subsequently. The best individual in the last generation is chosen to be the optimal design.

### C. Validation in Simulation

The optimal design was simulated in MATLAB (R2022a, Mathworks, Natick, MA) to validate its performance and compare it against the model of the Columbia exoskeleton. The Utah exoskeleton is shown to have a reduced range of motion (Table I). Notably, although the range of rotation for bending was not included in the cost function, the optimal design attained a reasonable motion range for bending in the frontal plane. More importantly, the Utah design exhibits a better transmission efficiency (i.e., lower condition number of the Jacobian matrix), not only at the upright pose, but also throughout the entire workspace. As compared to the Columbia exoskeleton, the condition number of the Jacobian matrix is consistently lower for poses that are on the three anatomical planes (Figure 3).

TABLE I  
COMPARISON OF RANGES OF ROTATION OF THE NECK EXOSKELETONS

Movement	Utah Design [ $^{\circ}$ ]	Columbia Design [ $^{\circ}$ ]
Flexion	45	45
Extension	15	15
Left Lateral Bending	20	25
Right Lateral Bending	20	25
Left Axial Rotation	32	45
Right Axial Rotation	32	50

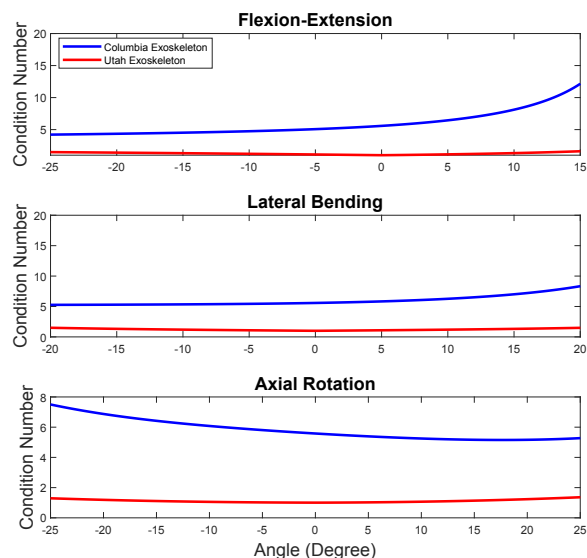


Fig. 3. Condition number of the Jacobian matrix in poses on each anatomical plane: (Top) sagittal plane, (Middle) frontal plane, and (Bottom) transverse plane. The Utah exoskeleton (red) has a lower condition number at the same robot configurations than the Columbia exoskeleton (blue).

### D. Physical Prototype

We realized this optimal computer model into a physical prototype. As noted earlier, the structural limitations in the Columbia exoskeleton were also caused by using joints that were made of low-profile components and linkages that were susceptible to bending, in addition to a poor transmission efficiency. In the physical realization of the Utah neck exoskeleton (Figure 4), we have also addressed these limitations.

The new linkage design uses an I-beam structure to improve their rigidity. I-beam structures are excellent at resisting bending moments in the plane of the web (the vertical element in its cross-section) while maintaining a small overall dimension. We designed the new linkages such that the webs are in the same plane of expected bending moments. These linkages were then 3D-printed (Pro 3, Raise 3D Technologies Inc.) using PLA.

There are two types of joints in the exoskeleton structure: revolute and spherical. In the Columbia exoskeleton, the revolute joints were realized by mating low-profile binding posts with bushing joints, but the fit was too loose. In the Utah exoskeleton, this was mitigated by press fitting machined shafts into precise ball bearings. Previously, the spherical joints were realized by combining a universal joint in series

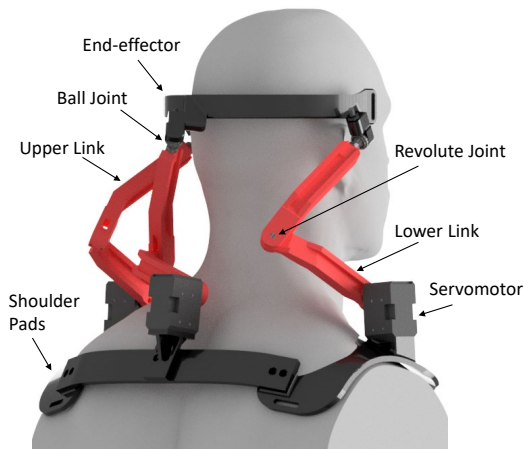


Fig. 4. Computer-aided design (CAD) rendering of the Utah neck exoskeleton.

with a revolute joint. Small plastic universal joints were used because they provide a large swivel range ( $\pm 45^\circ$ ). However, these plastic joints were manufactured such that there is slop within the mechanism. Instead, in the Utah exoskeleton, we used metal ball joints which are more precise, but have a smaller swivel range ( $\pm 22.5^\circ$ ). To avoid reducing the exoskeleton workspace, we aligned the ball joints such that the ball stud is centered to the socket in the upright neutral configuration.

The end effector (head attachment) and the base (shoulder attachment) were also redesigned based on the optimization result. Compared to the Columbia exoskeleton where the spherical joints were all behind the head (Figure 1), two of the spherical joints are located more laterally, which was reflected in the new end-effector design. Additionally, the Utah exoskeleton allowed the motors to be attached much lower and closer to the base (shoulder pads) which enhances the structural stability as well as reducing the overall size. The end effector is padded with foam and attached to the wearer's head via an adjustable strap. Additionally, the 'U' shape of the end-effector allows it to be slightly flexible and accommodate, to a limited degree, different head sizes.

### III. EXPERIMENTS

We conducted two experiments to evaluate the performance of the Utah neck exoskeleton in this paper. In the first experiment, we evaluated the rigidity of the Utah exoskeleton at multiple robot configurations. In the second experiment, we tested the usability of the Utah exoskeleton for a future study in ALS patients with severe head drop.

#### A. Bench-top Testing

The base of the exoskeleton was fixed to an inertial frame within the workspace of a multi-camera motion capture system (Vero 1.3, Vicon, Oxford Metrics, UK). Infrared markers were placed on the base and the end-effector so that the movement of the exoskeleton can be measured. A force-torque sensor (mini-45, ATI Industrial Automation, Apex,

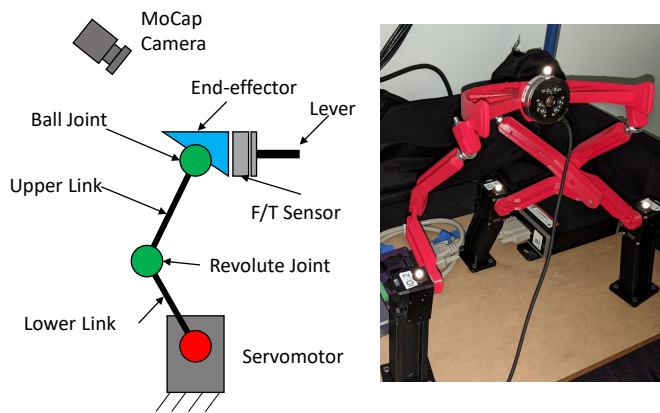


Fig. 5. setup of the bench-top experiment.

NC) was placed on the end-effector (Figure 5) to measure any external force applied on the end-effector via a lever.

The exoskeleton was held at multiple poses by locking the three servomotors (Dynamixel XM430-w350-r, ROBOTIS Inc. South Korea). A pulling force (normal to the X-Y plane of the force/torque sensor) was manually applied on the end-effector through the lever. Using the force-torque sensor, the amplitude of this force can be observed. The exoskeleton was positioned in the upright neutral configuration and at both the maximum and minimum angles shown in Table II in each plane, resulting in seven total poses. The data collection at each pose was repeated three times. Each time, we slowly increased the pulling force from 0 to 10 N on the end-effector and maintained at 10 N for 3 seconds before slowly removing the force. The maximum displacement of the end effector was used to quantify the structural stability of the design.

As a comparison, We strengthened the mechanical components (linkages and joints) of the Columbia neck exoskeleton in the same way we did in the Utah exoskeleton. However, once we mounted the force/torque sensor, the Columbia exoskeleton could not balance the weight of the sensor consistently by locking the actuated joints. Therefore, we excluded the Columbia exoskeleton from this bench-top experiment.

#### B. User Demonstration

In this paper, we invited a healthy volunteer to evaluate the usability of the Utah exoskeleton for a future study in ALS patients with severe head drop. The experiment has been approved by the Institutional Review Board (IRB) at the University of Utah.

Surface electromyography (EMG) activity was measured (Ultium, Noraxon, Scottsdale, AZ) on four of the participant's neck muscles: left and right sternocleidomastoid (SCM) and splenius capitis. The participant was seated in front of a computer screen on which two avatars were displayed (Figure 6). The avatar with a solid color indicated the target motion while the translucent avatar mirrored the actual head-neck motion of the participant, measured by the exoskeleton. A three-axis, analog mini joystick was used by the participant to

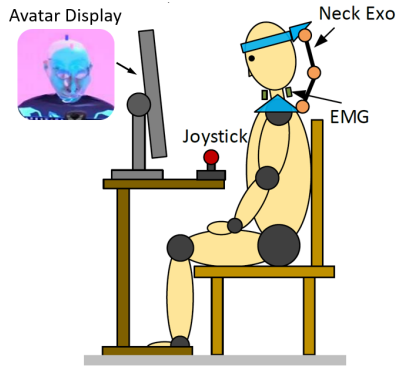


Fig. 6. (Top) Schematic of the experimental setup. (Bottom) The healthy subject performing a series of movements indicated by an avatar on the computer screen while wearing the Utah neck exoskeleton. Surface EMG was used to record the activity of the SCM and SC neck muscles.

control the speed of the neck exoskeleton. Similar controllers have been used in our previous studies [10].

TABLE II  
EXPERIMENTAL MOVEMENTS

Movement	Min Angle [Deg]	Max Angle [Deg]
Flexion-Extension	-25	15
Lateral Bending	-20	20
Axial Rotation	-25	25

The participant was given several minutes to become familiarized with the operation of the neck exoskeleton in both the assistive and measurement modes. In the assistive mode, the participant used the joystick to control the exoskeleton which was powered by the servomotors to assist their head-neck motions. In the measurement mode, the participant performed head-neck motions under their own power, while the exoskeleton measured the head angles through the motor encoders (the torques are disabled). Similar to the Columbia exoskeleton, the Utah exoskeleton is highly back-drivable when the motor torques are disabled. The participant was then instructed to follow the movement of the target avatar as closely as possible in three movements: flexion-extension in the sagittal plane, lateral bending in the frontal plane, and axial rotation in the transverse plane. The target avatar followed a sinusoidal movement (0.1 Hz) between the minimum and maximum angles outlined in Table II. EMG data (sampled at 2000 Hz) was time synchronized to kinematic data (sampled at 100 Hz) recorded by the motor encoders. The same process was repeated for both measurement and assistive modes.

## IV. RESULTS

The bench-top experiment characterized the structural stability of the Utah exoskeleton. Under the externally applied force (10 N) in the tested poses, the average displacements of the end-effector are summarized in Table III. The Utah exoskeleton is not completely rigid, but the displacements due to linkage deflections are small (<3 mm). Notably, the Columbia exoskeleton was unable to support itself sufficiently to provide meaningful data even with stronger mechanical linkages and joints.

TABLE III  
RIGIDITY TEST RESULT

Configuration	Mean (Standard Deviation) [mm]
Upright	0.6 (0.25)
Flexion 25°	1.2 (0.48)
Extension 15°	1.9 (0.54)
Left Bending 20°	3.1 (0.28)
Right Bending 20°	2.2 (0.69)
Left Rotation 25°	2.5 (0.15)
Right Rotation 25°	0.5 (0.18)

The user demonstration results illustrate the usability of the Utah neck exoskeleton. From a kinematic standpoint, the participant was able to achieve the desired trajectories across all movements (flexion-extension, lateral bending, and axial rotation), with and without the assistance provided by the neck exoskeleton. For example, while tracking a pure flexion-extension motion in the sagittal plane, the participant exhibited good tracking in the primary motion (Figure 7 Top) in both operating modes. However, without assistance, the participant showed a variable pattern of error in other anatomical planes. With assistance, the participant had less error in other planes (Figure 7 Middle) but may sustain constant error due to error in their operation on the joystick (Figure 7 Bottom).

Muscle EMG was also recorded during the experiment from four muscles. The raw EMG signals were band-pass filtered (3~20 Hz) and rectified. Figure 8 shows the processed EMG at the four muscles during sagittal-plane flexion-extension in the two experiment conditions (assisted vs. unassisted). The muscle activation of this healthy participant shows slight reduction in the peak EMG for left and right splenius capitis muscles when assisted by the Utah neck exoskeleton. Overall, the muscle EMG reduces slightly in all three movements when assisted by the Utah exoskeleton.

## V. DISCUSSION

During the optimization, there appears to be a clear trade-off between designs with a high range of rotation and a low condition number in the Jacobian matrix. Designs with a high range of rotation tend to also have high condition numbers and vice versa. In this paper, we chose to prioritize a design with a lower condition number to address the major limitation of the Columbia exoskeleton. This was also reflected in selecting the weights for the cost function during the optimization process.

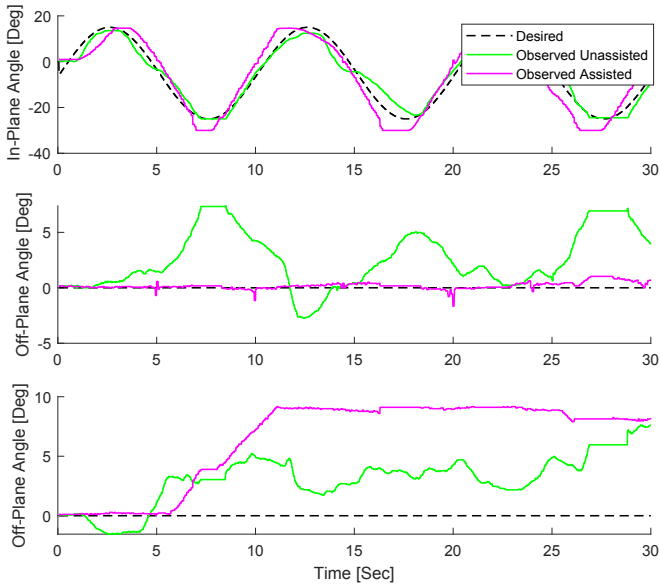


Fig. 7. Kinematic data during flexion-extension of the healthy subject. (Top) Desired (black dashed), observed unassisted (green), and observed assisted (magenta) movement of the head-neck in the sagittal plane. The out-of-plane movements of the head-neck are shown in the frontal plane (middle) and transverse plane (bottom).

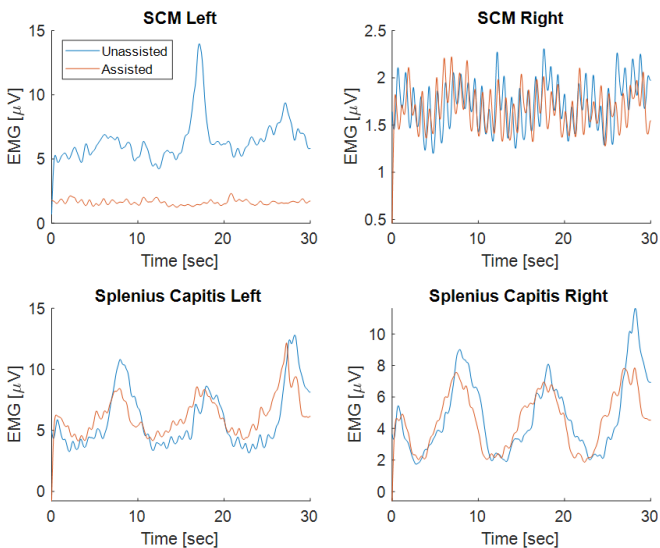


Fig. 8. EMG activity of the healthy participant during flexion-extension.

The optimization algorithm tended to maximize the distance between each spherical joint ( $A_i$ ). This can be explained because  $A_i$  points that are farther away from the geometric center of the end effector allow for a larger moment arm when applying torque to the head. Another design insight from the optimization is how the middle joints are oriented. In the optimized design, the axes of the middle joints are nearly perpendicular to each other to maximize force transmission throughout configurations within the exoskeleton workspace. Additionally, a design with a low condition number in the upright neutral configuration tended to have a low condition number throughout the entire workspace.

In the bench-top experiment, we applied a force (10 N) on the end-effector which is equivalent to  $\sim 1/5$  of the weight of the head [12]. In a previous study [21], we have demonstrated that a 10 N force would be sufficient to perturb the head from its nominal position in young healthy adults, suggesting that an external force of 10 N would likely be sufficient to support the head. With this 10 N force in our experiment, the Utah exoskeleton exhibited excellent structural stability as the displacement of the end-effector from its nominal pose is minimal. By contrast, the Columbia exoskeleton could not be held to a static pose by locking the actuators which explains why it would fail to support the head for patients with complete head drop.

The testing with a single healthy participant demonstrated the usability of the Utah exoskeleton and evaluated a potential future experimental protocol. This paves the way for us to continue our evaluation of the Utah neck exoskeleton with patients who suffer from severe ALS-associated head drop. In future studies with ALS patients, we plan to solicit patient feedback to further improve our neck exoskeleton. Working with a multidisciplinary ALS clinic at the University of Utah Hospital, we have contacted multiple patients with ALS head drop and they all are very enthusiastic about the Utah neck exoskeleton and willing to participate in our future studies.

## VI. CONCLUSION

This paper presented the design of a new neck exoskeleton (Utah exoskeleton) with improved structural stability, as compared to the previous Columbia exoskeleton. This was accomplished by a multi-objective optimization which maximized for both range of rotation and transmission efficiency. The physical construction was also enhanced through stronger and more precise linkages and joints. The ultimate goal of this research is to translate the neck exoskeleton technology to homes to improve quality of life of patients with ALS-associated head drop. With the improved structural stability, we are well-positioned to evaluate the Utah neck exoskeleton in patients with severe ALS head drop.

## VII. ACKNOWLEDGMENT

We thank the University of Utah for the new investigator start-up fund to conduct this research. We also thank Dr. Mark Bromberg and his colleagues for inviting us to learn from and work with the multidisciplinary ALS clinic at the University of Utah Hospital.

## REFERENCES

- [1] S. Pinto and M. De Carvalho, "Motor responses of the sternocleidomastoid muscle in patients with amyotrophic lateral sclerosis," *Muscle & Nerve: Official Journal of the American Association of Electrodiagnostic Medicine*, vol. 38, no. 4, pp. 1312–1317, 2008.
- [2] M. Sonoo, S. Kuwabara, T. Shimizu, T. Komori, F. Hirashima, A. Inaba, Y. Hatanaka, S. Misawa, Y. Kugio, and T. M. N. E. S. Group, "Utility of trapezius emg for diagnosis of amyotrophic lateral sclerosis," *Muscle & nerve*, vol. 39, no. 1, pp. 63–70, 2009.
- [3] M. C. Kiernan, S. Vucic, B. C. Cheah, M. R. Turner, A. Eisen, O. Hardiman, J. R. Burrell, and M. C. Zoing, "Amyotrophic lateral sclerosis," *The lancet*, vol. 377, no. 9769, pp. 942–955, 2011.
- [4] A. Walling, "Amyotrophic lateral sclerosis: Lou gehrig's disease," *American family physician*, vol. 59, no. 6, p. 1489, 1999.

- [5] J. D. Brodell Jr, A. Sulovari, D. N. Bernstein, P. C. Mongiovi, E. Ciafaloni, P. T. Rubery, and A. Mesfin, "Dropped head syndrome: an update on etiology and surgical management," *JBJS reviews*, vol. 8, no. 1, p. e0068, 2020.
- [6] S. Pinto and M. De Carvalho, "Motor responses of the sternocleidomastoid muscle in patients with amyotrophic lateral sclerosis," *Muscle & Nerve: Official Journal of the American Association of Electrodiagnostic Medicine*, vol. 38, no. 4, pp. 1312–1317, 2008.
- [7] S. Baxter, H. Reed, Z. Clarke, S. Judge, N. Heron, A. Mccarthy, J. Langley, A. Stanton, O. Wells, G. Squire *et al.*, "Evaluating a novel cervical orthosis, the sheffield support snood, in patients with amyotrophic lateral sclerosis/motor neuron disease with neck weakness," *Amyotrophic Lateral Sclerosis and Frontotemporal Degeneration*, vol. 17, no. 5-6, pp. 436–442, 2016.
- [8] L. Sproson, V. Lanfranchi, A. Collins, S. K. Chhetri, N. Daly, M. Ennis, L. Glennon, G. Gorrie, E. Jay, R. Marsden *et al.*, "Fit for purpose? a cross-sectional study to evaluate the acceptability and usability of headup, a novel neck support collar for neurological neck weakness," *Amyotrophic Lateral Sclerosis and Frontotemporal Degeneration*, vol. 22, no. 1-2, pp. 38–45, 2021.
- [9] H. Zhang and S. K. Agrawal, "Kinematic design of a dynamic brace for measurement of head/neck motion," *IEEE Robotics and Automation Letters*, vol. 2, no. 3, pp. 1428–1435, 2017.
- [10] —, "An active neck brace controlled by a joystick to assist head motion," *IEEE Robotics and Automation Letters*, vol. 3, no. 1, pp. 37–43, 2017.
- [11] H. Zhang, B.-C. Chang, P. Kulkarni, J. Andrews, N. A. Shneider, and S. Agrawal, "Amyotrophic lateral sclerosis patients regain head-neck control using a powered neck exoskeleton," in *2022 9th IEEE RAS/EMBS International Conference for Biomedical Robotics and Biomechatronics (BioRob)*. IEEE, 2022, pp. 01–06.
- [12] K. Ono, A. Kikuchi, M. Nakamura, H. Kobayashi, and N. Nakamura, "Human head tolerance to sagittal impact—reliable estimation deduced from experimental head injury using subhuman primates and human cadaver skulls," *SAE Transactions*, pp. 3837–3866, 1980.
- [13] A. Lozano, M. Ballesteros, D. Cruz-Ortiz, and I. Chairez, "Active neck orthosis for musculoskeletal cervical disorders rehabilitation using a parallel mini-robotic device," *Control Engineering Practice*, vol. 128, p. 105312, 2022.
- [14] M. E.-H. Ibrahim, M. T. El-Wakad, M. S. El-Mohandes, S. A. Sami *et al.*, "Implementation and evaluation of a dynamic neck brace rehabilitation device prototype," *Journal of Healthcare Engineering*, vol. 2022, 2022.
- [15] A. Koszulinski, F. Ennaiem, J. Sandoval, L. Romdhane, and M. A. Laribi, "Optimal design and experimental validation of a cable-driven parallel robot for movement training of the head–neck joint," *Robotics*, vol. 12, no. 1, p. 18, 2023.
- [16] D. Wu, L. Wang, and P. Li, "A 6-dof exoskeleton for head and neck motion assist with parallel manipulator and semg based control," in *2016 International Conference on Control, Decision and Information Technologies (CoDIT)*. IEEE, 2016, pp. 341–344.
- [17] R. Di Gregorio, "The 3-rrs wrist: a new, simple and non-overconstrained spherical parallel manipulator," *J. Mech. Des.*, vol. 126, no. 5, pp. 850–855, 2004.
- [18] H. Zhang, *A novel robotic platform to assist, train, and study head-neck movement*. Columbia University, 2019.
- [19] J. Pusey, A. Fattah, S. Agrawal, and E. Messina, "Design and workspace analysis of a 6–6 cable-suspended parallel robot," *Mechanism and machine theory*, vol. 39, no. 7, pp. 761–778, 2004.
- [20] J. P. Merlet, "Jacobian, Manipulability, Condition Number, and Accuracy of Parallel Robots," *Journal of Mechanical Design*, vol. 128, no. 1, pp. 199–206, 06 2005.
- [21] H. Zhang, V. Santamaria, and S. Agrawal, "Applying force perturbations using a wearable robotic neck brace," in *2020 IEEE/RSJ International Conference on Intelligent Robots and Systems (IROS)*. IEEE, pp. 4197–4202.